Author(s): Lindén, J. & Lippmaa, M. & Miettinen, J. & Tittonen, I. & Katila, T. & Karppinen, Maarit & Niinistö, L. & Nara, A. & Yamauchi, H.

Title: Precise determination of the hyperfine parameters of europium in multifluorite perovskites by 151Eu Mössbauer spectroscopy

Year: 1994

Version: Final published version

Please cite the original version:

Lindén, J. & Lippmaa, M. & Miettinen, J. & Tittonen, I. & Katila, T. & Karppinen, Maarit & Niinistö, L. & Nara, A. & Yamauchi, H. 1994. Precise determination of the hyperfine parameters of europium in multifluorite perovskites by 151Eu Mössbauer spectroscopy. Physical Review B. Volume 49, Issue 21. 15280-15286. ISSN 1550-235X (electronic). DOI: 10.1103/physrevb.49.15280.

Precise determination of the hyperfine parameters of europium in multifluorite perovskites by ^{151}Eu Mössbauer spectroscopy

J. Lindén, M. Lippmaa, J. Miettinen, I. Tittonen, and T. Katila
Department of Technical Physics, Helsinki University of Technology, FIN-02150 Espoo, Finland

M. Karppinen and L. Niinistö
Laboratory of Inorganic and Analytical Chemistry, Helsinki University of Technology, FIN-02150 Espoo, Finland

A. Nara and H. Yamauchi
International Superconductivity Technology Center, Tokyo, Japan
(Received 29 December 1993)

The hyperfine interactions at the europium lattice sites in samples of the homologous (Fe,Cu)Sr_2(Eu,Ce)$_n$$Cu_2O_{4+2n+z}$ ($n = 2, 3$) series were studied by ^{151}Eu Mössbauer spectroscopy. The work was motivated by the search for new superconducting phases. This homologous series is based on the $YBa_2Cu_3O_{7-\delta}$ (1:2:3) structure. The samples used in the Mössbauer measurements consisted of crystallites with random orientation and grain oriented crystallites. The texture of oriented samples was analyzed by x-ray diffraction. The complete quadrupole Hamiltonian of the 21.5-keV γ-transition of ^{151}Eu was successfully applied in the analyses of all the Mössbauer spectra. In samples having $n \leq 2$ the europium atoms occupy a single lattice site, whereas the spectra of the $n = 3$ samples exhibit hyperfine interactions of the two different europium sites. Analyzing the hyperfine parameters of the latter samples was made possible by simultaneous fitting of three spectra, corresponding to three different crystal orientations of the same specimen. This fitting scheme also enables more precise determination of the hyperfine parameters in the $n = 2$ samples. In these samples an electric field gradient (EFG), with a large negative-valued main component (V_{zz}) parallel with the crystal c axis, was found. In the $n = 3$ samples, the two EFG's of the europium sites were found to have V_{zz} components of opposite signs. The negative V_{zz} value was attributed to the rare-earth site adjacent to the CuO layer. This site, found in all samples of the series, corresponds to the rare-earth site of the 1:2:3 system.

I. INTRODUCTION

The search for new high-T_c superconducting materials is often based on using existing families of compounds to synthesize new related compositions, which may exhibit superconducting properties. Usually, the chemical syntheses involve changing the number of simple building blocks within the unit cell. A representative example is the Bi-based phases ($Bi_2Sr_2Ca_{n-1}Cu_nO_{2n+4}$) in which the amount of Ca-Cu-O units may vary.[1] Characterizing the physical properties of the various phases should give information about the mechanisms leading to the superconducting transition.

The $YBa_2Cu_3O_{7-\delta}$ (1:2:3) system has served as the parent phase for the newly synthesized homologous series (Fe,Cu)Sr_2(Eu,Ce)$_n$$Cu_2O_{4+2n+z}$.[2-4] The first member of the series ($n = 1$) is the tetragonal 1:2:3 phase. Higher members include a triple perovskite block and $[(Eu,Ce)O_2]_{n-1}$ fluorite blocks. So far superconductivity has not been detected when $n > 2$. The crystal structures of the $n = 2$ and 3 phases of the series are shown in Fig. 1.

The hyperfine interactions of the rare-earth site of the 1:2:3 compounds are now quite well known due to extensive ^{151}Eu Mössbauer studies.[5-15] The shapes of the spectra are adequately explained by a nonzero electric quadrupole interaction, the Hamiltonian of which is readily implemented for computer fitting.[15] The closely related Eu-doped Ca site of the 80 K phase of the Bi series has also been studied in some detail.[15-17] The values of the hyperfine interactions at the Eu site have been found

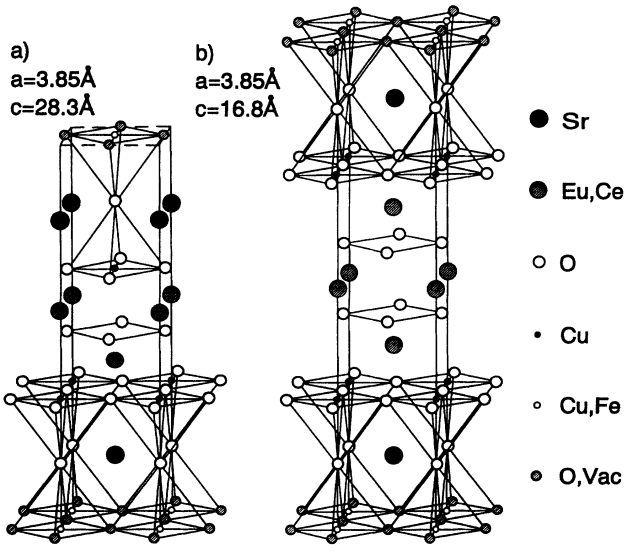

FIG. 1. Crystal structures of two members of the (Fe,Cu)Sr_2(Eu,Ce)$_n$$Cu_2O_{4+2n+z}$ series ($n = 2$ and 3).

to be similar due to the resemblance of the rare-earth sites in these compounds. A large electric field gradient (EFG), having a negative main component (V_{zz}) parallel with the crystal c axis and a substantial asymmetry parameter, has been found to prevail at the Eu ion, which has the 3+ oxidation state. The asymmetry parameter of the EFG (η) is defined as[18]

$$\eta = \frac{|V_{yy}| - |V_{xx}|}{|V_{zz}|}, \quad (1)$$

where the potential derivatives are expressed in the principal axis coordinate system and $|V_{zz}| > |V_{yy}| > |V_{xx}|$.[18] The sign of V_{zz} can be obtained since the quadrupole interactions make the resonance line slightly asymmetric. If, however, η is exactly 1, the resonance is completely symmetric and only $|V_{zz}|$ may be obtained.

Samples of $(Fe_xCu_{1-x})Sr_2(Eu_{1/2}Ce_{1/2})_2Cu_2O_9$ and $(Fe_xCu_{1-x})Sr_2(Eu_{1/3}Ce_{2/3})_3Cu_2O_{11}$ were used in the present work. These correspond to $n = 2$ and 3 in the general $(Fe,Cu)Sr_2(Eu,Ce)_nCu_2O_{4+2n+z}$ formula, which includes the $(Fe,Cu)Sr_2(Eu,Ce)O_{6+z}$ (1:2:3) structure and $n-1$ fluorite blocks. The oxygen contents may vary a little but z is usually close to 1. Our aim was to characterize the hyperfine interactions at the rare-earth sites by ^{151}Eu Mössbauer measurements. In the computer fittings of the spectra the complete electric quadrupole Hamiltonian was used. In the $n = 2$ series, an EFG similar to that of the 1:2:3 compounds was found, i.e., a negative-valued V_{zz} parallel with the c axis. For the $n = 3$ series two EFG's originating in the two nonequivalent lattice sites of Eu were observed. The main components of the gradients were of opposite signs and parallel with each other. The negative V_{zz} value corresponds to the site found in the perovskite block of 1:2:3 compounds, while the positive V_{zz} comes from the fluorite block. All of the Eu ions are in the 3+ oxidation state.

The relative intensities of the Mössbauer lines vary when the angle between the direction of the γ rays and the quantization axis is varied. In order to utilize this effect single crystal absorbers are needed. Another possibility is to use oriented powder crystallites. Orientation of the high-T_c phases is achieved by submitting the powders to a strong magnetic field, which interacts with the magnetic moments of the crystallites, forcing them to align with the field. The samples were oriented in two different directions, which made possible several unique measurements of the same sample. This enabled fitting of the two field gradients, having overlapping spectral components, since more detailed data were obtained. The aligned specimens were found to orient with their crystal c axes parallel with the external magnetic field. A quantitative texture analysis of the oriented samples was done using x-ray diffraction.

II. EXPERIMENTAL DETAILS

The preparation of the samples followed the scheme of Ref. 4. In brief, a solid state reaction of high-purity powders of Eu_2O_3, CeO_2, Sr_2CO_3, Fe_2O_3, and CuO was used. The mixed powders were pressed and annealed at 900–1070 °C at an oxygen pressure of 1–3 atm. The annealing was repeated after grinding the samples. The purity of the samples thus obtained was checked using x-ray powder diffraction (Cu $K\alpha$ radiation). Contrary to the pure 1:2:3 structure iron is needed to stabilize the formation of pure phases, the optimum concentration being close to $x = 0.75$. The following iron concentrations were used: $x = 0.5$, 0.625, 0.75, 0.875, and 1.0 for the $n = 2$ samples and $x = 0.375$, 0.5, 0.625, 0.875, and 1.0 for the $n = 3$ samples. The presence of iron also enables probing of the copper (iron) lattice sites with ^{57}Fe Mössbauer spectroscopy.[19]

Room-temperature Mössbauer spectra were recorded in transmission geometry. The data were gathered until the unfolded background level reached at least 10^6 counts. A standard 100-mCi ^{151}Sm:Sm_2O_3 source was used. The 21.5-keV γ quanta were detected with a scintillation detector equipped with a 3-mm-thick NaI crystal. The linear periodic Doppler modulation used in the measurements had a maximum velocity of 4 mm/s. A maximum velocity of 20 mm/s was applied to check for Eu ions in the 2+ oxidation state. The thickness of the absorber samples was 20 mg/cm^2, corresponding to the ^{151}Eu thicknesses of 1.8 mg/cm^2 and 1.5 mg/cm^2 for the $n = 2$ and $n = 3$ series, respectively.

Magnetically aligned samples for Mössbauer measurements were prepared by letting epoxy-soaked powders harden in an 11.7-T magnetic field. The alignment direction was chosen either parallel with or perpendicular to the face of the samples. The directions of the crystal axes in oriented samples were also checked by x-ray diffraction. A Philips MPD 1880 x-ray diffractometer was used. With this setup only Bragg planes parallel with the sample surface are reached, since both the sample and the detector are automatically rotated during the 2θ scan (θ-2θ geometry). This keeps the angles between the sample surface and the incident and refracted rays equal. An INEL CPS 120 facility was later used to improve the texture analysis.[20] This enabled x-ray diffraction measurements with the incident beam set at selected angles (20°–40°) with respect to the sample surface.

III. RESULTS AND DISCUSSION

The powder x-ray diffraction data confirmed the purity of the $n = 2$ and $n = 3$ phases. The observed diffraction lines of both phases could be labeled with Miller indices.[4] In Fig. 2, x-ray data of an $n = 2$ sample are shown. The first spectrum (a) was recorded from a random crystallite sample, while the two other spectra (b) and (c) originate from magnetically aligned samples. In spectrum (b) the direction of the external magnetic field was parallel with the face of the sample, while in (c) the field was perpendicular to it. The c axis clearly tends to align parallel with the magnetic field. The alignment, however, is not perfect which can be seen through the existence of reflections with nonzero h and k indices in Fig. 2(c) and nonzero l reflections in Fig. 2(b). The reflections indicated a tetragonal unit cell. The a lattice parameter increased from 3.839(2) Å to 3.850(5) Å as a function of

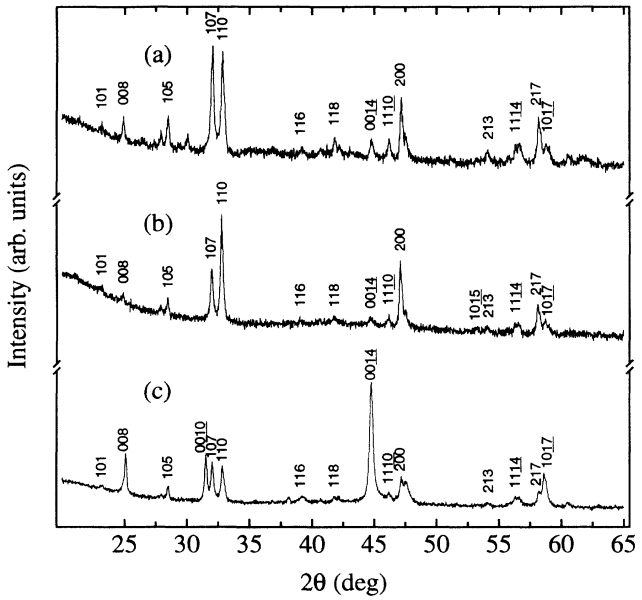

FIG. 2. X-ray diffraction patterns of samples of $(Fe_{0.75}Cu_{0.25})Sr_2(Eu_{1/2}Ce_{1/2})_2Cu_2O_9$ for powdered (a) and oriented (b), (c) specimens. The sample was oriented with the magnetic field parallel with (b) and perpendicular to (c) the sample face.

x, while the c parameter decreased from 28.455(0) Å to 28.190(2) Å, yielding an almost constant unit cell volume.

In Fig. 3, the x-ray data of the $n = 3$ phase are shown. The magnetically aligned samples also oriented with their crystal c axes parallel with the magnetic field, which is seen as an enhancement of the $00l$ reflections in Fig. 3(c) and the $hk0$ reflections in Fig. 3(b). These samples were also found to be tetragonal. The lattice parameters showed a similar dependence on the iron contents as the $n = 2$ samples. The a lattice parameter increased from 3.835(6) Å to 3.840(1) Å while the c parameter decreased from 16.893(6) Å to 16.756(2) Å.

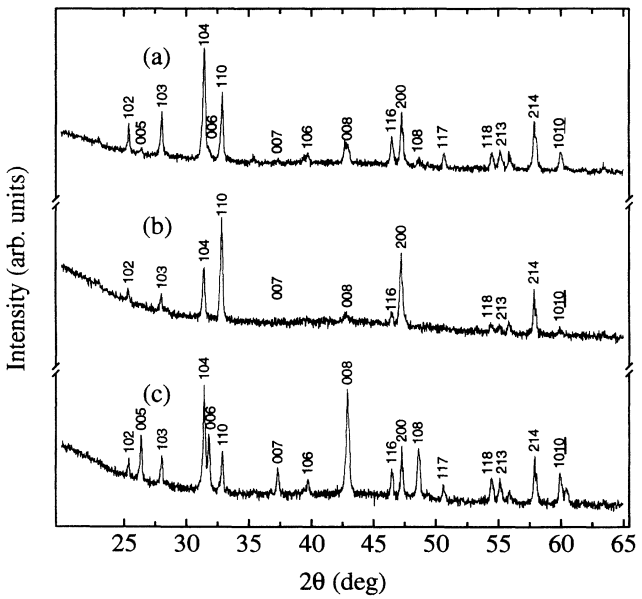

FIG. 3. X-ray diffraction spectra of samples of $(Fe_{0.625}Cu_{0.375})Sr_2(Eu_{1/3}Ce_{2/3})_3Cu_2O_{11}$ for powdered (a) and oriented (b), (c) specimens. The sample was oriented with the magnetic field parallel with (b) and perpendicular to (c) the sample face.

A. Analysis of the texture effects

To check the reliability of the orientatinal effects obtained in fittings of Mössbauer spectra x-ray texture analyses were performed. The aim was to use the intensities of the various observed x-ray peaks to calculate the distribution of the angle θ (measured between the crystal c axis and the normal of the sample surface). Since the line intensities of the x-ray peaks depend on several factors, the line intensities of spectra of magnetically oriented samples were divided by the line intensities of the corresponding random crystallite spectra. The relative line intensity distribution which was thus obtained should exhibit pure texture effects. The various θ angles were calculated with the aid of purely geometrical considerations, presented in the Appendix.

The angular distributions of crystallites in two oriented specimens of $(Fe_{0.625}Cu_{0.375})Sr_2(Eu_{1/3}Ce_{2/3})_3Cu_2O_{11}$ are shown in Fig. 4. The direction of the external magnetic field was perpendicular to the sample surface in Fig. 4(a) and parallel with the surface in Fig. 4(b). The distributions were fitted with a function consisting of a Gaussian curve and a constant background. The dotted lines are error estimates. The distributions indicate that only some of the crystallites align with the magnetic field while others remain unaffected.

In ^{151}Eu Mössbauer spectra the line intensities are proportional to $\frac{1}{2}\sin^2\theta$ or $\frac{1}{4}+\frac{1}{4}\cos^2\theta$ (if the principal z axis coincides with the c axis and the γ rays enter the sample surface perpendicularly).[15] For absorbers with random orientation of the crystallites the intensity factors must be averaged over the 4π solid angle, yielding values equivalent with those of an absorber consisting of crystallites oriented in the so-called magic angle ($\theta \simeq 54.74°$). The average θ value obtained in the Mössbauer fits may also be calculated by averaging the Mössbauer intensity factors multiplied by the θ-angle distributions, obtained from the texture analysis, over a 4π solid angle. The average angles obtained from four analyzed specimens are presented in Table I.

B. Analysis of Mössbauer spectra

In all of the ^{151}Eu Mössbauer spectra a broadened resonance line, typical of an unresolved quadrupole interaction, was observed. The position (center shift) of the line indicated that Eu exists only in the 3+ oxidation state. No traces of the 2+ oxidation state were seen in measurements using higher Doppler velocities. The spectra were fitted using the full quadrupole Hamiltonian of the excited $I' = \frac{7}{2}$ and ground $I = \frac{5}{2}$ spin states. For the $n = 2$ samples the following fit parameters were used (one-site fitting): spectral base line (Y_D), total absorp-

TABLE I. The average degree of orientation obtained from texture analysis of x-ray diffraction spectra.

Orientation	n	x	Average θ
H|| surface	2	0.75	$56(^{+7}_{-1})^\circ$
H$\perp$ surface	2	0.75	$45(^{+7}_{-11})^\circ$
H|| surface	3	0.625	$64(^{+5}_{-4})^\circ$
H$\perp$ surface	3	0.625	$45(^{+7}_{-11})^\circ$

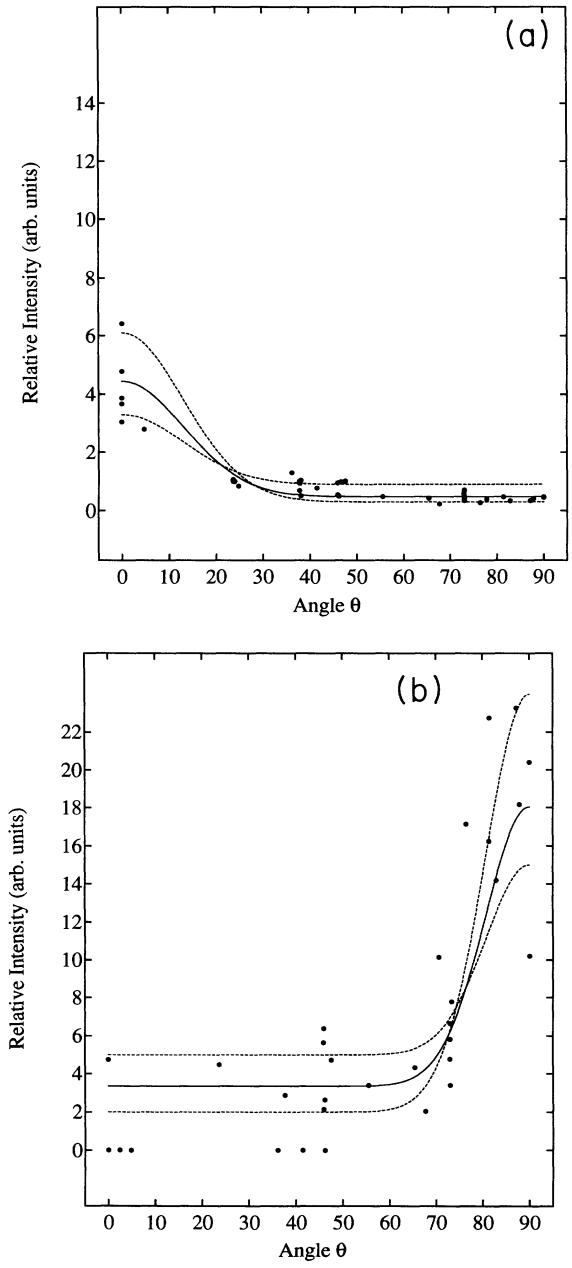

FIG. 4. Distribution of orientation angle θ (in degrees) for two $(Fe_{0.625}Cu_{0.375})Sr_2(Eu_{1/3}Ce_{2/3})_3Cu_2O_{11}$ specimens oriented (a) with the magnetic field perpendicular to the sample surface and (b) with the magnetic field parallel with the surface. The distributions were obtained from x-ray diffraction spectra.

tion (T), center shift (S), V_{zz}, η, the angle between γ rays and V_{zz} (θ), and one common linewidth (Γ) for all spectral components. When fitting the spectra of the $n = 3$ samples, an additional set of V_{zz}, η, and S was added to the fit parameters, due to the existence of two hyperfine-split components (two-site fitting). The following values for the quadrupole moments of the excited and the ground states were used: $Q_e = 1.50 \times 10^{-28}$ m^2 and $Q_g = 1.14 \times 10^{-28}$ m^2, respectively.[21]

When analyzing spectra of random-orientation crystallites θ was fixed to the magic angle (54.74°). For magnetically aligned crystallites θ was never fixed, since according to x-ray measurements the alignment is not perfect, yielding θ values far from the two possible extremes of 90° and 0°.

In order to obtain reliable results, two or three spectra corresponding to the same specimen oriented in various directions were fitted simultaneously. Only Y_D, T, and θ were specified separately for each spectrum, the rest of the parameters being in common. The χ^2 parameter describing the goodness of the fit always acquired values corresponding to 1.00(4).

1. $n = 2$ samples

In Fig. 5, results from simultaneously fitted Mössbauer spectra of three specimens of the

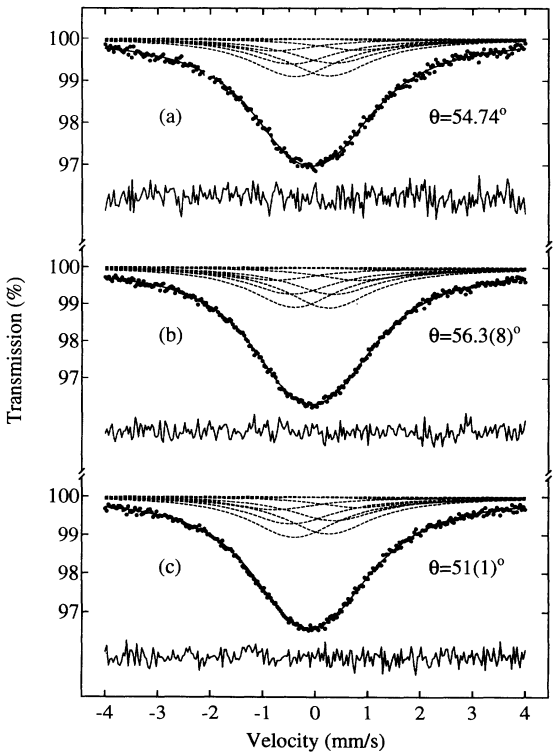

FIG. 5. Simultaneously fitted Mössbauer spectra of $(Fe_{0.75}Cu_{0.25})Sr_2(Eu_{1/2}Ce_{1/2})_2Cu_2O_9$ samples: (a) random orientation, (b) c axis oriented perpendicular to the γ beam, and (c) c axis oriented parallel with the γ beam. The obtained values for θ, the spectral components, and the difference between data and fit are shown for each spectrum.

TABLE II. The average degree of orientation (θ) obtained from multiple fittings of Mössbauer spectra of the $n = 2$ series.

x	θ (**H**|| surface)	θ (**H**$\perp$ surface)
0.5	55(1)°	51(1)°
0.625	57(1)°	51(2)°
0.75	56.3(8)°	51(1)°
0.875	–	50(2)°
1.0	–	52(1)°

TABLE III. The hyperfine parameters as a function of x for the $(Fe_xCu_{1-x})Sr_2(Eu_{1/2}Ce_{1/2})_2Cu_2O_9$ samples.

x	eQ_gV_{zz} (mm/s)	η	S (mm/s)	Γ (mm/s)
0.5	-4.31(14)	0.98(4)	-0.056(5)	2.07(4)
0.625	-4.48(4)	0.82(6)	-0.050(3)	2.11(5)
0.75	-4.66(3)	0.83(4)	-0.050(2)	2.042(4)
0.875	-4.19(24)	0.98(7)	-0.052(5)	2.10(7)
1.0	-4.33(17)	0.92(5)	-0.064(6)	2.05(5)

$(Fe_{75}Cu_{0.25})Sr_2(Eu_{1/2}Ce_{1/2})_2Cu_2O_9$ sample are given. The 12 components of the quadrupole-split spectra are shown on top of each spectrum. The value of θ, obtained from the fitting, is also given for each spectrum. The θ values obtained from Mössbauer spectra of all $n = 2$ samples are shown in Table II. They agree with the results from x-ray texture analysis results.

Negative initial values were used for V_{zz} in all the fittings. Assuming V_{zz} to be positive increased the value of χ^2 and made $\eta > 1$. It also yielded θ values according to which V_{zz} would be perpendicular to the c axis. Due to the tetragonal crystal symmetry this is, however, highly improbable, as is seen, e.g., from point-charge calculations.

The EFG parameters (eQ_gV_{zz} and η) did not exhibit any clear functional dependence on x; see Table III. It is noteworthy that the statistical errors were smallest for the parameters obtained from the $x = 0.75$ sample. The linewidth of the $x = 0.75$ sample was also the smallest, 2.042(4) mm/s. This indicates that the phase purity is best when $x = 0.75$.

2. $n = 3$ samples

At first glance obtaining physically correct fittings of the Mössbauer data of $n = 3$ samples seems impossible due to the broad resonance line of the ^{151}Eu 21.5-kev γ transition, covering the hyperfine interactions prevailing at the two Eu sites. When attempting fittings of single spectra using two sets of hyperfine parameters this was in fact the case, since $\chi^2 = 1.0$ was obtained for a variety of parameter values. Therefore the following scheme was adopted. First it was noted from one-site fittings of all the $n = 3$ samples that η always tended to be ≥ 1.0.

Then with the aid of computer simulations it was shown that a Mössbauer spectrum consisting of two EFG's of approximately equal magnitude and spectral intensity yield an η close to 1.0 in a single EFG fitting, when the two V_{zz} parameters are of opposite signs. If the two V_{zz} parameters are of the same sign, a single EFG fitting results in a V_{zz} and η close to the average of the two EFG's. The results obtained by fitting the simulated spectra with an single EFG are shown in Table IV.

The parameters used to generate the two simulations were $Y_D = 2 \times 10^6$, $\Gamma = 2.0$ mm/s, $eQ_gV_{zz}^{(1)} = 5.5$ mm/s, $\eta^{(1)} = 0.0$, $T^{(1)} = 2.5$ %, $eQ_gV_{zz}^{(2)} = \pm 4.0$ mm/s, $\eta^{(2)} = 0.6$, $T^{(2)} = 5.0$%, and $S^{(1)} = S^{(2)} = 0.02$ mm/s.

Single EFG fitting of the measured and simulated data thus suggests that the two EFG tensors prevailing at the two Eu sites have V_{zz} parameters of opposite signs. Also simple point-charge calculations indicated that the two rare-earth sites have EFG's with V_{zz} parameters of opposite signs. Furthermore the calculations revealed that the directions of the two V_{zz} parameters coincide with the crystal c axis, which is consistent with the lattice symmetry of the Eu sites in these compounds.

We thus decided that the spectra from the $n = 3$ samples should be fitted with two parallel V_{zz} parameters of opposite signs. Simultaneous fitting of spectra, from specimens of parallel, perpendicular, and random geometry, was used. The relative intensity of the lines of the two sites depend on Eu contents of the rare-earth sites. We assumed the Eu atoms to be randomly distributed on the rare-earth sites and fixed the line intensities according to the occurrence of the two sites: i.e., $\frac{1}{3}$ for the fluorite site and $\frac{2}{3}$ for the perovskite site. The negative-valued V_{zz} was assumed to arise from the familiar perovskite site, resembling those found in $n = 1$ and 2 samples. The positive-valued V_{zz} was attributed to the fluorite site. The center shifts of the two sites were set equal. The hyperfine parameters obtained, are presented in Table V. The θ-values obtained are shown in Table VI. They agree well with the results obtained with the x-ray texture analysis; see Table I.

Assuming the fluorite site to be subjected to the negative-valued V_{zz} increased χ^2. Also the direction of V_{zz} with respect to the c axis changed from parallel to perpendicular.

TABLE IV. Hyperfine parameters obtained by single EFG fittings of simulated spectra. The parameter values used to generate the simulations are given in the text.

Initial V_{zz} signs	eQ_gV_{zz} (mm/s)	η	S (mm/s)	Γ (mm/s)
$V_{zz}^{(1,2)} > 0$	4.5(3)	0.5(1)	0.023(7)	1.98(8)
$V_{zz}^{(1)} > 0$ $V_{zz}^{(2)} < 0$	-3.7(4)	1.1(1)	0.020(7)	2.07(1)

TABLE V. The hyperfine parameters as a function of x for the $(Fe_xCu_{1-x})Sr_2(Eu_{1/3}Ce_{2/3})_3Cu_2O_{11}$ samples, obtained by simultaneous fitting of multiple spectra with two EFG's.

x	$eQ_gV_{zz}^{(1)}$ (mm/s)	$\eta^{(1)}$	$eQ_gV_{zz}^{(2)}$ (mm/s)	$\eta^{(2)}$	S (mm/s)	Γ (mm/s)
0.375	-4.43(7)	0.57(2)	5.5(3)	0.00(5)	-0.077(5)	1.896(5)
0.5	-4.0(1)	0.60(7)	5.5(3)	0.00(2)	-0.064(3)	1.95(3)
0.625	-4.3(6)	0.9(2)	4(1)	0.0(7)	-0.074(6)	1.98(5)
0.875	-4.0(3)	0.5(1)	5.3(6)	0.0(6)	-0.072(6)	1.94(5)
1.0	-4.8(3)	1.00(8)	3.7(6)	0.2(7)	-0.053(9)	1.90(5)

IV. CONCLUSIONS

In this work the hyperfine interactions of the rare-earth sites in the $n = 2$ and 3 phases of the homologous $(Fe,Cu)Sr_2(Eu,Ce)_nCu_2O_{4+2n+z}$ series were measured. With the aid of magnetically aligned samples and simultaneous fittings of multiple spectra the precision for determining the hyperfine parameters was substantially enhanced. For the $n = 2$ and 3 phase an EFG, with a large negative V_{zz} and a nonzero asymmetry parameter, similar to that of the rare-earth site in the 1:2:3 compound was found. An additional EFG with a positive V_{zz} and a zero asymmetry parameter was found in the $n = 3$ samples. This EFG was shown to prevail at the fluorite site found in phases with n greater than 2. The analysis was entirely based on simultaneous fitting of three spectra recorded from two magnetically oriented samples and one random powder sample of the same material. The EFG parameters obtained were not sensitive to the iron contents, suggesting that iron mainly enters the Cu(1) site and leaves the Cu(2) site unaltered. This is also the case in the 1:2:3 system.[22] The center shift, which reflects the s-electron density at the nucleus, was constant as well. The statistical errors and the linewidth were smallest for the sample with $x = 0.75$, reflecting its optimum stoichiometry.

The x-ray patterns revealed that the c axes of powder crystallites in both phases align in the direction of an external magnetic field. The texture analysis also yielded average orientation angles in agreement with the results obtained from the Mössbauer fits. The degree of orientation was somewhat larger for the $n = 3$ samples than for the $n = 2$ samples.

ACKNOWLEDGMENTS

Financial support from the Academy of Finland (M.L.) and the following foundations are gratefully acknowledged: Emil Aaltonen Foundation (J.L., I.T., and M.L.), The Finnish Science Foundation (J.L.), and the Scandinavia-Japan Sasakawa Foundation (M.K. and A.N.). The Institute of Chemical Physics and Biophysics of the Estonian Academy of Sciences is acknowledged for providing the magnet in the orienting experiments. Dr. Y. Kawate of the Cryogenic Technology Center and the Kobe Steel Company of Japan are acknowledged for their assistance in performing HIP treatments.

TABLE VI. The average degree of orientation (θ) obtained from multiple fittings of Mössbauer spectra of the $n = 3$ series. The orientational degree for random samples was fixed at 54.74°.

x	θ (H|| surface)	θ (H$\perp$ surface)
0.375	71(4)°	44(5)°
0.5	59(3)°	28(6)°
0.625	57(4)°	46(5)°
0.875	60(6)°	41(6)°
1.0	70(4)°	45(3)°

APPENDIX

In x-ray patterns measured with the Philips MPD 1880 facility (θ-2θ geometry) all the observed Bragg reflection planes are parallel with the sample surface. Therefore the angle θ between the c axis and the plane normal is simply

$$\cos\theta = \frac{l}{c}\frac{1}{\sqrt{(\frac{h}{a})^2+(\frac{k}{b})^2+(\frac{l}{c})^2}}, \tag{A1}$$

where $d^{-1} = \sqrt{(\frac{h}{a})^2+(\frac{k}{b})^2+(\frac{l}{c})^2}$ is the spacing between the planes. The distribution of the c axes in various directions is thus readily obtained once the Miller indices have been identified.

If, however, the Bragg planes are tilted at an angle α with respect to the sample surface, the θ angles are no longer single valued. This is the case when using the INEL CPS 120 facility. The situation is illustrated in Fig. 6. Taking the direction of the d vector as the z axis a vector $\mathbf{c}$ parallel with the c axis may be expressed as

$$\mathbf{c} = c\cos\theta\mathbf{k} + c\sin\theta(\cos\phi\mathbf{i} + \sin\phi\mathbf{j}), \tag{A2}$$

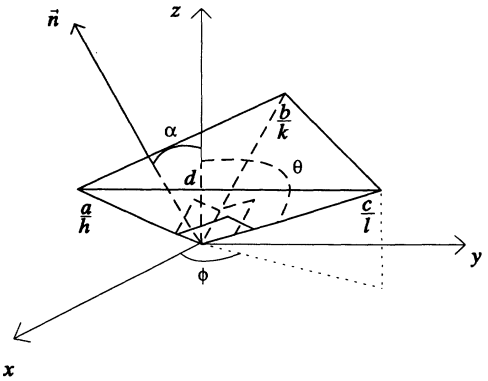

FIG. 6. Geometry of a single hkl reflection from a Bragg plane tilted at an angle α with respect to the sample surface.

where θ is obtained from Eq. (A1) and ϕ describes rotation of the c axis in plane normal to the z axis. The vector representation of the normal to the sample surface may be chosen as

$$\mathbf{n} = \cos\alpha\mathbf{k} - \sin\alpha\mathbf{j}. \tag{A3}$$

If the distribution of the ϕ angle is isotropic (in our experiments achieved by rotating the sample in a plane perpendicular to $\mathbf{n}$ during the measurement), the average angle between the c axis and $\mathbf{n}$ (denoted as $\bar{\theta}$) is

$$\bar{\theta} = \frac{1}{2\pi}\int_0^{2\pi} \arccos\left(\frac{\mathbf{n}\cdot\mathbf{c}}{c}\right) d\phi. \tag{A4}$$

For pure $00l$ reflections this integral simply yields $\bar{\theta} = \alpha$, since in this case $d = \frac{c}{l}$.

The θ values used in the texture analysis where calculated according to the formulas (A1) and (A4).

[1] P. Bordet, J. Capponi, C. Chaillout, J. Chenavas, A. Hewat, E. Hewat, J. Hodeau, and M. Marezio, Stud. High Temp. Supercond. **2**, 885 (1988).

[2] T. Wada, A. Ichinose, H. Yamauchi, and S. Tanaka, Physica C **171**, 344 (1990).

[3] T. Wada, A. Ichinose, and S. Tanaka *Advances in Superconductivity III* (Springer, Tokyo, 1991), p. 303.

[4] T. Wada, A. Nara, A. Ichinose, H. Yamauchi, and S. Tanaka, Physica C **192**, 181 (1992).

[5] M. Eibschutz, D. W. Murphy, S. Sunshine, L. G. Van Uitert, S. M. Zahurak, and W. H. Grodkiewicz, Phys. Rev. B **35**, 8714 (1987).

[6] J. M. D. Coey and K. Donnelly, Z. Phys. B **67**, 513 (1987).

[7] P. Boolchand, R. N. Enzweiler, I. Zitovsky, R. L. Meng, P. H. Hor, C. W. Chu, and C. Y. Huang, Solid State Commun. **63**, 521 (1987).

[8] A. Freimuth, S. Blumenröder, G. Jackel, H. Kierspel, J. Langen, G. Buth, A. Nowack, H. Schmidt, W. Schlabitz, E. Zirngiebl, and E. Mörsen, Z. Phys. B **68**, 433 (1987).

[9] E. Ikonen, J. Hietaniemi, K. Härkönen, M. Karppinen, T. Katila, J. Lindén, L. Niinistö, H. Sipola, I. Tittonen, and K. Ullakko, *High-T_c Superconductors* (Plenum, New York, 1988), p. 209.

[10] G. Wortman, S. Blumenöder, A. Freimuth, and D. Riegel, Phys. Lett. A **126**, 434 (1988).

[11] Z. M. Stadnik, G. Stroink, and R. A. Dunlap, Phys Rev. B **39**, 9108 (1989).

[12] Z. M. Stadnik, G. Stroink, and T. Arakawa, Phys Rev. B **44**, 12552 (1991).

[13] M. Lippmaa, E. Realo, and K. Realo, Phys. Lett. A **139**, 353 (1989).

[14] I. Tittonen, J. Hietaniemi, J. Huttunen, E. Ikonen, M. Karppinen, T. Katila, J. Lindén, and L. Niinistö, Hyperfine Interact. **55**, 1399 (1990).

[15] J. Lindén, M. Lippmaa, I. Tittonen, J. Hietaniemi, E. Ikonen, T. Katila, T. Karlemo, M. Karppinen, L. Niinistö, and K. Ullakko, Phys. Rev. B **46**, 8534 (1992).

[16] W. A. Groen, R. Steens, H. W. Zanderbergen, M. W. Dirken, F. M. Mulder, and R. C. Thiel, J. Less Common Met. **155**, 133 (1989).

[17] F. W. Oliver, L. May, and C. E. Violet, J. Appl. Phys. **67**, 5083 (1990).

[18] U. Gonser, in *Mössbauer Spectroscopy*, edited by U. Gonser (Springer, New York, 1975), Vol. 5, p. 27.

[19] A. Nara *et al.* (unpublished).

[20] Instrumentation électronique curved position sensitive 120° detector.

[21] J. G. Stevens, in *Handbook of Spectroscopy*, edited by J. W. Robinson (CRC, Boca Raton, 1981), p. 209.

[22] P. Boolchand and D. McDaniel, Hyperfine Interact. **72**, 125 (1992).